POD GENERATOR PROJECT, A NUMERICAL ASSESSMENT OF THE INSPECTION OF FATIGUE CRACKS USING TOFD

A. W. F. Volker, J. G. P. Bloom
TNO Science and Industry, P.O. Box 155, 2600 AD Delft, The Netherlands

Abstract

Risk based inspection strategies rely on detailed knowledge of the performance of inspection techniques. The objective of the "POD generator" project is to develop a numerical modeling approach to assess effectiveness of specific inspection techniques. Simulation offers flexibly and reliability at acceptable costs. Therefore numerical models have been developed and validated for accurately simulating the physics of inspection techniques. These numerical models are then used to generate quantitative probability of detection (POD) curves. In the case of ultrasonic time-of-flight-diffraction (TOFD) inspections, the human factor is included at two levels. First in the way a TOFD scan is carried out (positioning variations). And secondly, in the fact that simulated inspection results are interpreted by real operators.

This paper shows the assessment of the inspection of fatigue cracks using TOFD using this numerical approach. The influence of gas inclusions and the human interpretation on the performance of the inspection was investigated by generating multiple POD-curves under different circumstances. This way we show that the numerical modeling approach is an efficient and reliable way of determining the required effort to inspect welds for fatigue cracks under different circumstances.

1. POD Generator project, a modeling approach

The maintenance of – often very complex – production installations in the chemical industry and the oil and gas sector is of paramount importance for these companies due to aspects of safety, production loss and reputation. Therefore such installations are inspected on a regular basis, carried out by skilled personnel using advanced nondestructive techniques. Timing of these inspections and locations is based on experience and also imposed by law, as degradation is often not visible and the locations are often difficult to reach.

Risk based inspection (RBI) strategies rely on detailed knowledge of the performance of inspection techniques, together with detailed knowledge and experience of the degradation of an installation, in order to quantitatively assess the risks associated with both detected and undetected defects. A widely used measure for inspection reliability, and thus more or less its effectiveness, is the probability of detection (POD), i.e. the probability a defect of a certain kind and size will be detected under certain circumstances. As plant owners constantly have to make a tradeoff between the performance and cost of an inspection technique, a thorough insight in the performance of an inspection technique is very important.

Figure 1 The POD Generator Project modeling approach.

It is well known that every inspection technique has limitations with respect to POD. Moreover, a POD is influenced by many factors. Apart from the technique itself, it depends on many and varied aspects such as the inspection procedure, the defect and object geometry and technique specific material conditions (and properties) like for example surface roughness and grain size for ultrasonic techniques. And last-but-not-least a POD depends on the inspectors applying a technique, i.e. the so-called human factor.

For several years now [1, 2], a number of chemical plant and pipeline owners as well as inspection service companies in The Netherlands are participating in a joint industry project named the "POD generator" project. The objective of this project is to develop a numerical modeling approach allowing flexible and reliable assessment of the inspection effectiveness for a specific situation, in terms of POD, yet at a fraction of the costs necessary for empirical assessment.

Besides the models to simulate various degradation mechanisms, e.g. crack growth and corrosion, numerical models have been and are being developed and validated for accurately simulating the physics of various inspection techniques, currently ultrasonic inspection techniques (TOFD, PE and GW). Also the human factor is taken into account, either by translating human influences into physical parameters and chance factors, which are included in the models, or mostly by applying human interpretation to the simulated inspection results. The interpreted simulated inspection results are then used to generate quantitative POD curves for the specific technique and circumstances under study.

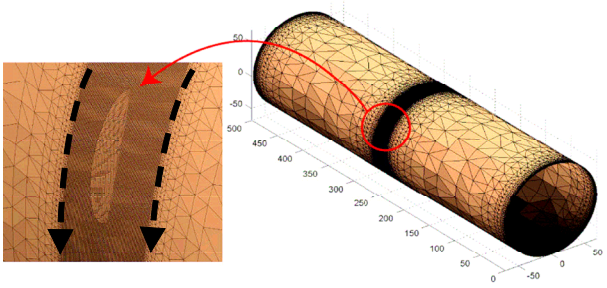

Figure 2 Pipe morphology mesh showing a small fatigue crack at the weld root.

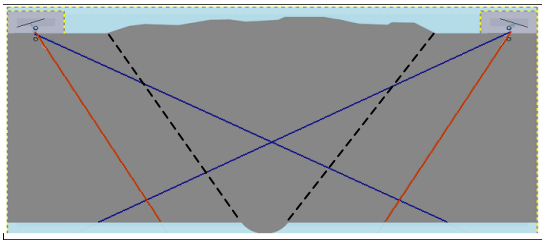

Figure 3 Typical TOFD probe setup at adjacent sides of a weld. Note weld cap and root.

In previous work [3] the validation of the different models and the general approach was discussed in more detail. This paper focuses on the generation of POD's for ultrasonic TOFD inspections of pipe welds with internal surface breaking fatigue cracks. Here we demonstrate the possibilities and advantages of the POD generator by calculating POD's for different inspection parameters and levels of an important influencing factor of TOFD inspections: high-low.

2. POD Generator for TOFD inspection of fatigue cracks

The POD generator for simulated TOFD inspection of pipes subjected to fatigue degradation consists of the following three modules.

- A degradation module, which generates simulated pipe morphologies that degrade over time due to the growth of root fatigue cracks in the girth welds.

- An inspection module, which generates B-scans resulting from simulated TOFD inspection of the welds.
- A POD curve calculation module, which estimates POD curves based on the human interpreted TOFD inspection results and the list of simulated defects.

The degradation module models the growth of root cracks from initial faults in the girth welds. The number of initial faults per weld is an input parameter of the degradation module. The growth rate of the root cracks is driven by the amount and the frequency of loading applied to the pipe, which are also input parameters. The root cracks are positioned at or near the weld root and grow from the inner wall of the pipe.

To make the simulated TOFD inspection results more realistic, an important factor for realistic human interpretation, the presence of grains in the steel and surface roughness are included in the inspection model. The grains were implemented by locally varying the material properties inside the weld (see Figure 4). These small variations lead to noise in the inspection result. The size of the grains and amount of material properties (ΔC_p,ΔC_s) variations are input parameters. The surface roughness is implemented by giving the actual surface of the pipe wall a varying height. It is determined by two parameters: the amplitude of the variations and the spatial frequency content of the variations. For an even higher realism, the following factors are also included in the inspection module: weld cap and weld root, porosities, weld high-low and small random variations of ultrasonic probe position and separation. The parameters of the random variations of the ultrasonic probe were determined by analyzing inspection data provided by the inspection service companies. Although the simulations are carried out in 2D, a pseudo 3D simulation result is obtained by applying inverse imaging on the final B-scans. The collection of a number of 2D simulations in the B-scan can be seen as an imaged 3D dataset, i.e. the diffraction hyperbolas are collapsed into a single point. The inverse imaging procedure essentially spreads the energy over the diffraction hyperbolas and so producing a pseudo 3D dataset. The opening angle of the transducer is taken into account as well and essentially limits the spatial extent of this hyperbola. This can be seen in the bottom of Figure 4.

The pipes modeled in the degradation module are imported into the inspection module to model the inspection of the welds. The welds are inspected using a TOFD setup which consists of a source and a receiver placed on both sides of the weld. The simulated inspection is carried out along the circumference of the welds with a small stepsize of 1 mm. At every inspection point a simulation of the full elastic wavefield is carried out using the commercially available UMASIS software. The responses for all probe positions are combined into a B-scan, which reveals the indications of the simulated defects as for example fatigue cracks, porosities and grain noise.

Next, the simulated B-scans are interpreted by experienced and certified TOFD operators from different companies using their own software, i.e. in exactly the same way as if it were real TOFD B-scans obtained in the field. This way, the human factor is realistically taken into account. Of course, the interpreting operators do not know the location of simulated defects nor the type of defects or the number of defects present per B-scan. These values also vary per B-scan. The only information given to the operators are the TOFD inspection parameters necessary for the sizing of defects detected by them in the B-scans.

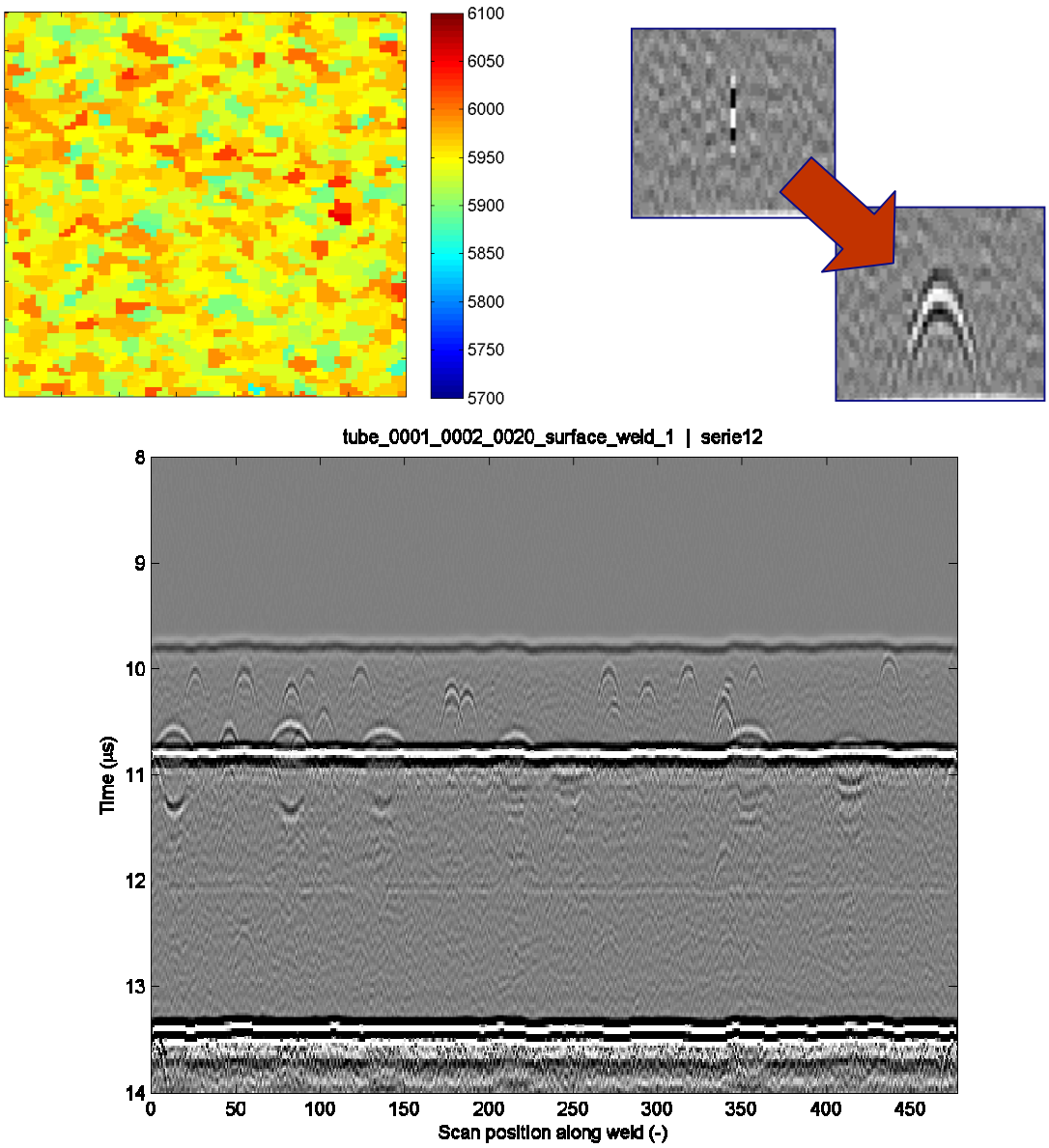

Figure 4. The top left graph shows the pressure wave speed of the model inside the weld. It consists of grains which all have a different velocity. The size of the grains and velocity differences can be changed. The top right graph shows the result of the inverse imaging step where pseudo 3D modeling results are generated. The bottom graph shows the resulting B-scan.

The result of this human interpretation of the simulated TOFD B-scans is a list of all found indications per B-scan, including position, height and length of the defect. By comparing this list and the list with the real properties of the simulated defects from the degradation model, the POD curve can be calculated. For the calculation of the POD the continuous signal response model (a-hat-versus-a) is used, using software by Annis [3].

3. TOFD Inspection performance in various situations

For the first set of POD curves it was decided to use configurations that generate realistic but still ideal B-scans. They are ideal in the sense that they do not contain any complicating factors for the interpretation. These factors will be addressed in a separate case to study the effect of these complications on the POD independently. For the first 6 cases for the POD curves, the inspection parameters were derived from the TOFD procedure [5,6] which suggests inspection parameters as function of wall thickness values.

The procedure leaves some room for the choice of specific parameters. Three typical wall thicknesses were chosen and the optimal inspection parameters for this wall thickness were derived from this procedure. For each wall thickness a second case was defined where one parameter was varied. This resulted in the six basic cases shown in Table 1. These cases allow the investigation of the influence of a specific parameter on the POD curve.

After the basic POD curves were generated, the influence of complicating factors on the POD curves was determined. From discussions with the sponsors one of the complicating factors for TOFD data interpretation is high-low. POD curves were generated for different levels of these complicating factors. For the case of high low this means that POD curves (with the same parameters as case 3) were calculated with a high-low level of 0.5, 1.0 and 1.5 mm. This way multi-parameter POD's were calculated that depend on the defect height as well as the level of the complications. This gives insight in how sensitive the inspection is for the complicating factors.

TABLE 1. OVERVIEW OF THE DIFFERENT INSPECTION PARAMETERS FOR THE DIFFERENT POD CASES.

Case	**1**	**2**	**3**	**4**	**5**	**6**	**7**	**8**	**9**
WT (mm)	8	8	12	12	25	25	12	12	12
Frequency (MHz)	7.5	7.5	10	5	5	5	5	5	5
Beam angle (deg)	70	70	70	70	70	70	70	70	70
Element size (mm)	3	6	3	6	3	6	6	6	6
High-low (mm)	0	0	0	0	0	0	1,5	0,5	1
# Slag inclusion (1/m)	0	0	0	0	0	0	0	0	0

POD Curves of Ideal Cases 1 – 6

For each specific case and dataset a POD curve was calculated. Each dataset was interpreted by three operators, which results in six POD curves per case, so a total amount of 18 POD curves for the basic TOFD cases. The following analysis can be performed on the resulting set of POD curves:

- Influence on inspection parameter choice on POD
- Influence human-factor on POD

To compare the results more quantitatively the following three points were extracted from each POD curve:

- A50, defect height at 50% POD
- A90, defect height at 90% POD
- A90/95, defect height at 90% POD with 95% confidence level

The unit of all these points is mm. These numbers determine the POD curve and therefore describe the performance of the inspection. The smaller the number, the better is the performance of the inspection. The left graph of Figure 5 shows bar-plots of the A50, A90, and A90/95 points as function of the TOFD case number obtaining from a single operator. The only difference between case 1 and case 2 is the diameter of the probe (3 mm for case 1 and 6 mm for case 2). The fact that the A50, A90 and A90/95 values are approximately the same, the crystal diameter has no influence on the performance of the TOFD inspection.

The changed parameter between case 3 and case 4 is the frequency. Case 3 is the inspection of a 12 mm thick wall with 10 MHz and case 4 is the inspection of a 12 mm thick wall with 5 MHz. The higher the frequency the smaller the wavelet, the better the

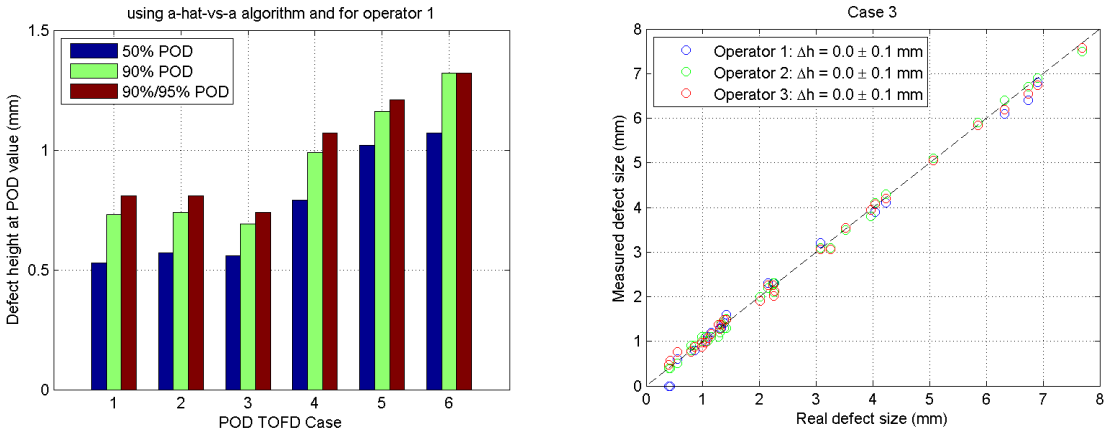

Figure 5. Comparison of the values of the A50, A90 and A90/95 points of the POD curves for the different TOFD cases. The left graph shows a comparison for the POD curves for the first six cases. The right graph shows a comparison between the different operators.

defect can be discerned from the back-wall reflection. This also follows from the POD curves of both cases. The noise from the grains inside the weld strongly increases with frequency, which would result in a lower POD. Conclusion from this case would be that the positive effect on the POD due to the smaller wavelet, is stronger than the negative effect causes by the increased noise.

The changed parameter between case 5 & 6 is again the probe diameter (3 mm and 6 mm respectively). Again no influence on POD is observed. The difference between case 4 & 6 is the wall thickness. From the POD curves follows that a thicker wall has a higher POD (i.e. lower performance). This can be explained by the longer sound paths in the object of inspection, which results in a worse signal to noise ratio..

The right graph of Figure 5 shows the sizing performance of the three different operators for case 3. It shows the interpreted crack height as function of the real defect height. If no errors would be made, all points should be located on the dashed line. Several conclusions can be drawn from this graph. First, there is no offset and the sizing error is more or less constant over the used defect height range. Furthermore, the differences between the operators are very small. On average the differences between the operators was 0.1 mm.

Influence of High-Low on POD

In the cases 7 until 9 the amount of high-low was varied between 0.5 and 1.5 mm. High low occurs when the back wall of a plate or pipe has different levels on both sides on the weld. For example this can happen when two pipe segments are welded with a horizontal or vertical offset. The effect on the inspection is that the back-wall echo from both sides of the weld arrives at different times. This hinders the interpretation because the reflection of the tip echo of a defect is more difficult to separate from the back wall echo.

The effect of the complicating factors on the performance of the inspection technique should be compared to the acceptation level. If the POD is still well below this level, the effect can be ignored. According to [4], the acceptation level for a pipe with a WT of 12 mm is 1 mm (assuming defects are longer than 12 mm which is true for the defects simulated in the POD generator). Figure 6 shows the POD of a defect of 1 mm with increasing level of high-low (right graph). As can be seen the amount of high-low strongly influences the detection probability of a defect with a size the same as the acceptation level.

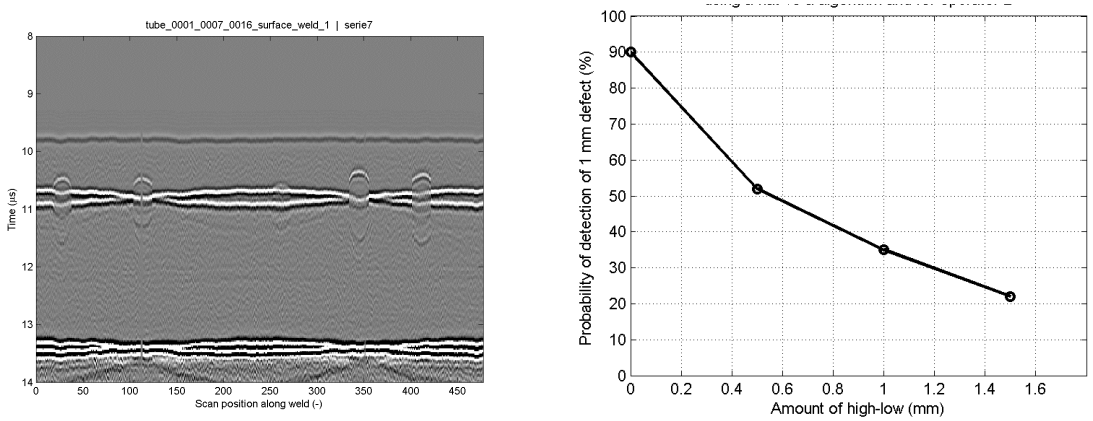

FIGURE 6. Comparison of the three POD points for increasing level of high-low. The left graph shows the result using the hit-miss algorithm and right graph the results for the a-hat-vs-a algorithm.

Influence of gas inclusions on POD

Gas inclusions are created during welding and are mostly located inside the weld. They are small air-filled bubbles with a size ranging from several micrometers to several millimeters. These holes lead to the point scatter like indications. Gas inclusions are implemented by adding a probability that at each inspection point one or more gas inclusions may occur. The gas inclusions are modeled as vacuum circled geometries. The probability that one or more gas inclusions occur is determined by the average number of inclusions per meter weld. The size of the gas inclusion is randomly determined from a lognormal distribution. This distribution is determined by two parameters: the average size of the gas inclusions and the standard deviation around this average. The gas inclusion always occurs in the weld itself. They have a higher probability to occur in the bottom of the weld. There is 50% chance that a gas inclusion occurs in the bottom of the weld, a 30% chance in the middle and a 20% chance in the top of the weld. Their axial position is uniformly distributed. The axial edges are determined by the weld angle.

In case 10 until 12 the number of gas inclusions per meter was increased from 25 per meter to 75 per meter. As expected, the â-vs-a dataset is not influenced by the amount of gas pores. The defects than can be found will still be correctly sized. The hit-miss dataset however is influenced by the amount of gas inclusions. When many gas inclusions are present in a B-scan more defects will be missed. This is also visible graphically in the left graph of Figure 7. Note that no false calls were observed. Also for this case the results are compared by investigating the probability to detect a defect with the same size as the acceptation level. Figure 8 shows the POD of a defect of 1 mm with increasing level of gas pores (right graph). The amount of gas pores decreases this probability, although less pronounced than with high-low.

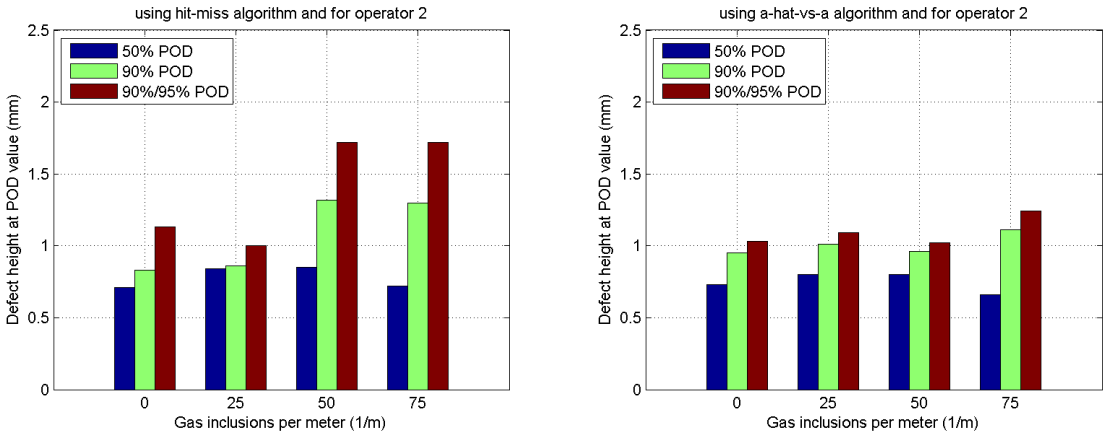

Figure 7. Comparison of the three POD points for increasing amount of gas pores. The left graph shows the result using the hit-miss algorithm and right graph the results for the a-hat-vs-a algorithm.

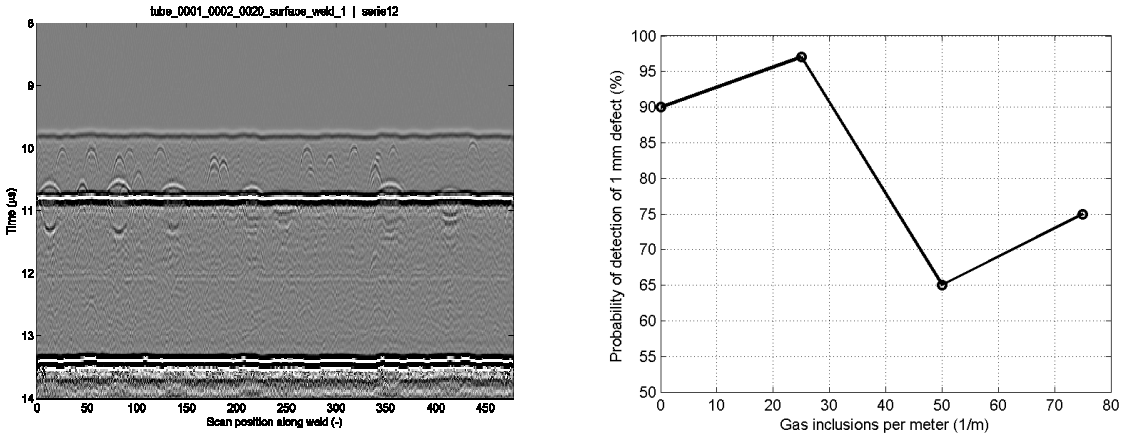

Figure 8. Comparison of the three POD points for increasing level of high-low. The left graph shows the result using the hit-miss algorithm and right graph the results for the a-hat-vs-a algorithm.

4. Conclusions and future plans

The POD generator was demonstrated for the TOFD inspection of girth welds. The POD generator can now be used to calculate POD curves for arbitrary inspection parameters (e.g. frequency, probe diameter, beam angle) under various conditions (e.g. different weld geometries, occurrence of gas pores, high-low). The human factor is taken into account by the interpretation of the B-scans.

To demonstrate how the POD generator works, various POD curves were generated. Six curves were calculated for standard inspections under good conditions. In the other six POD curves the influence of the occurrence of gas pores or high-low was shown.

The following conclusions can be drawn from the first six standard POD curves, calculated with the POD generator. First of all the choice of probe diameter has almost no influence on the POD curve. This was shown on the inspection on a pipe with a WT of 8 mm with 7.5 MHz and on a pipe with a WT of 25 mm with 15 MHz. The inspection frequency has a significant influence on the performance of a TOFD inspection. This was shown by the fact that there was a large difference on the POD curve between the inspection of pipe with a WT of 15 mm with 5 MHz and 10 MHz. The higher the frequency the smaller the wavelet, the better the defect can be discerned from the back-wall reflection. There was only a very small difference between the POD curves resulting

from the interpretation by two different operators. Therefore, the influence of the human factor on the POD curves was small.

The advanced POD curves showed how the POD generator can be used to investigate the influence of complicating factors on the performance of inspection techniques. Here, the influence of high-low and gas inclusions was investigated. From this numerical assessment followed that the probability of detection of a defect of 1 mm (acceptation level for the simulated cases) decreased from 90% at no high-low to 22% at a high-low level of 1.5 mm. In the case of gas pores the POD of a defect of 1 mm decreased from 90% when no gas pores were present, to 75% when on average 75 gas pores were present per meter.

In the future the POD generator will be used to investigate the sensitivity of inspection techniques to complicating factors. This will further help the industry to make well informed decisions. The datasets created in this project also allow a more detailed comparison of the different method that can be used to calculate the POD curve. This will also be carried out in the future.

Acknowledgements

We gratefully acknowledge the sponsors of the POD Generator Project for their financial and technical support as well as their invaluable advice: Applus RTD B.V., Lloyds Register, NAM, N.V. Nederlandse Gasunie, SABIC, SGS Nederland B.V., Shell Global Solutions, Total, Tronox.

References

1. A.W.F. Volker, F.H. Dijkstra, S. Terpstra, H.A.M. Heerings, M.A. Lont, “Modeling of NDE Reliability: Development of a POD Generator”, in *Proceedings of the 16th World Conference on Nondestructive Testing*, Montreal, 2004.
2. A. Mast, A.W.F. Volker, “POD Generator, A quantative assessment of the performance of inspection systems”, in *34th Review of Progress in Quantitative Nondestructive Evaluation*, editors D.O. Thompson and D.E. Chimenti, ISBN: 978-0-7354-0494-6; DOI:10.1063/1.2902641, AIP Conf. Proc. February 28, 2008 Volume 975, pp. 1701-1707.
3. J. G. P. Bloom, U. Stelwagen, A. Mast, A. W. F. Volker, A. H. M. Krom, A. A. Mohamoud, and G. P. Van Gils, “POD generator project, development of numerical modeling tools for quantitative assessment of the performance of non-destructive inspection techniques”, in *35th Review of Progress in Quantitative Nondestructive Evaluation*, AIP Conf. Proc. March 3, 2009 Volume 1096, pp. 1816-1823.
3. C. Annis, “Nondestructive Evaluation System Reliability Assessment”, Department of Defense (DoD) Handbook MIL-HDBK-1823, 28 February 2007, pp. 132.
4. M. Wall, F. A. Wedgwood, S. Burch, “Modelling of NDT reliability (POD) and applying corrections for human factors”, ECNDT '98, Copenhagen 26-29 May 1998, pp. 8.
5. “BS 7706, Guide to Calibration and setting-up of the Ultrasonic Time of Flight diffraction (TOFD) technique for defect detection, location and sizing of flaws”, British standard on TOFD, 1993. Summary at: http://www.ndt.net/article/tofd/bs_tofd/bs_tofd.htm
6. “ENV 583-6, Non-destructive testing - Ultrasonic examination - Part 6: Time-of-flight diffraction technique as a method for detection and sizing of discontinuities”, Draft European standard on TOFD, Also published as DIN EN 583-6, 2008-07. Summary at: http://www.ndt.net/article/tofd/env_tofd/env_tofd.htm